Low frequency azimuthal stability of the ionization region of the Hall thruster discharge. I. Local analysis

D. Escobar[1,a)] and E. Ahedo[2,b)]
[1]*Universidad Politécnica de Madrid, 28040 Madrid, Spain*
[2]*Universidad Carlos III de Madrid, 28911 Leganés, Spain*

(Received 12 January 2014; accepted 28 March 2014; published online 18 April 2014)

Results based on a local linear stability analysis of the Hall thruster discharge are presented. A one-dimensional azimuthal framework is used including three species: neutrals, singly charged ions, and electrons. A simplified linear model is developed with the aim of deriving analytical expressions to characterize the stability of the ionization region. The results from the local analysis presented here indicate the existence of an instability that gives rise to an azimuthal oscillation in the $+E \times B$ direction with a long wavelength. According to the model, the instability seems to appear only in regions where the ionization and the electric field make it possible to have positive gradients of plasma density and ion velocity at the same time. A more complex model is also solved numerically to validate the analytical results. Additionally, parametric variations are carried out with respect to the main parameters of the model to identify the trends of the instability. As the temperature increases and the neutral-to-plasma density ratio decreases, the growth rate of the instability decreases down to a limit where azimuthal perturbations are no longer unstable. © *2014 AIP Publishing LLC*. [http://dx.doi.org/10.1063/1.4870963]

I. INTRODUCTION

The Hall Effect Thruster (HET) is a type of electric propulsion device initially developed in the 1960s by both the USA[1] and the former USSR[2,3] independently. The development continued in the shadow in the USSR reaching a mature status in the 1970s and 1980s. In the 1990s, the advanced state of this Russian technology became known in western countries, which rapidly restarted the analysis and development of Hall thrusters. Nowadays, there are several companies manufacturing modern Hall thrusters for operational use in USA, Russia, and Europe. The main applications of these thrusters are low-thrust propulsion of interplanetary probes, orbital raising of satellites, and north-south station-keeping of geostationary satellites.[4] There are two basic variants of Hall thrusters, the Stationary Plasma Thruster (SPT) and the Thruster with Anode Layer (TAL), in Russian nomenclature. The main difference between them is the material of the walls of the devices, ceramic for the SPT model and metallic for the TAL.

The operation principle of a typical Hall thruster is as follows. A strong radial magnetic field is imposed together with an axial electric field inside a coaxial channel where a neutral gas, typically xenon, is introduced as propellant. Three species of particles are present in a HET: neutrals, which are injected from the rear part of the channel and flow axially towards the thruster exit; electrons, which are introduced by a cathode located just outside the channel and flow upstream towards the anode describing an $\mathbf{E} \times \mathbf{B}$ closed-drift in the azimuthal direction; and ions, which are created by ionization of neutrals due to collisions with the counter-streaming electrons and are accelerated axially by the electric field in the channel and the near plume. The magnetic field is such that electrons are strongly magnetized whereas ions are unmagnetized as the ion Larmor radius is much larger than the typical length of the thruster channel. For a given thruster, the main control parameters are the discharge voltage, the magnetic field, and the mass flow rate, being the discharge current an output of the dynamical system. For a given magnetic field and a given mass flow rate, it is possible to represent the evolution of the discharge current as a function of the discharge voltage in the so-called current-voltage (I–V) curve. This curve shows two distinct regimes separated by a knee: a low ionization regime, where the discharge current increases rapidly with the voltage; and a current saturated regime, where the discharge current is fairly insensitive to changes in the discharge voltage.

Over the last decade, great efforts have been dedicated by the HET community to the understanding of the physics of these devices. However, there are still some important aspects to clarify. Since the early stages of the Hall thruster technology development, it has been clear that the electron perpendicular conductivity inside the channel and in the plume is too high to be explained with classical collisional theories.[5] That is why the term anomalous diffusion is normally used to refer to the higher-than-expected electron axial current. The radial magnetic field and the axial electric field trap the electrons in an azimuthal closed-drift, and, according to classical theories, the only mechanism that allows the electrons to drift axially is the collisions with other species. However, the electron conductivity measured experimentally is between one and two orders of magnitude higher than the expected one from collisions, so another mechanism is suspected to enhance the electron mobility.

[a)]Ph.D. Candidate, Equipo de Propulsión Espacial y Plasmas. URL: http://aero.uc3m.es/ep2
[b)]Professor, Equipo de Propulsión Espacial y Plasmas. Electronic mail: eduardo.ahedo@uc3m.es

Although the experimental evidence is not unanimous, most common properties of the anomalous diffusion are (a) it is present in the whole channel as well as in the plume of the thruster;[6] (b) there is a dip of electron conductivity in the region of high magnetic and electric fields;[6–9] (c) the electron mobility scales as $1/B$, where B is the magnetic field strength;[10,11] and (d) the magnetic field gradients affect greatly the electron conductivity.[12]

Currently, there is no agreement within the Hall thruster community about the mechanism of the anomalous diffusion, but the most accepted explanations are two: plasma oscillations, referred to as Bohm-type or turbulent diffusion, based on the fact that correlated azimuthal oscillations of density and electric field can induce a net axial electron current;[13,14] and near-wall conductivity, where secondary electrons emitted by the walls can induce a net axial current.[15] However, near-wall conductivity does not seem to explain the anomalous diffusion since many simulation codes[16–18] that include a near-wall conductivity model still need a Bohm-type diffusion contribution to match the electron conductivity measured experimentally. On the other hand, several experiments have confirmed with various techniques the presence of azimuthal oscillations. These *azimuthal* oscillations are normally grouped into low frequency (5–30 kHz), medium frequency (30–100 kHz), and high frequency (1–10 MHz) oscillations. Many linear stability analyses carried out so far focus on the acceleration region or the high frequency range, where the ionization may be safely neglected. However, a set of experimental results show also the presence of low frequency azimuthal oscillations originated in the ionization region of the thruster.[14,19–21] The theoretical analysis of this oscillation, usually called spoke, is at the centre of the present study.

The paper is organized as follows. In Sec. II, a review of the available literature on low frequency oscillations is presented from three points of view: experiments, numerical simulations, and theoretical analyses. A linear stability analysis of azimuthal low frequency perturbations is carried out in Sec. III. In Sec. IV, a comparison against previous stability analyses is presented. Finally, Sec. V is devoted to conclusions.

II. REVIEW OF PREVIOUS STUDIES ON LOW FREQUENCY OSCILLATIONS

A. Experimental results

Back in the 1960s, Janes and Lowder[14] carried out a seminal work on low frequency azimuthal oscillations in HETs. Even though the Hall accelerator analysed in that research differs significantly from a modern HET, many of the conclusions are still valid. In that study, a spoke was detected by means of azimuthally separated Langmuir probes. This spoke appeared as a density variation rotating azimuthally in the $\mathbf{E}\times\mathbf{B}$ direction with a phase velocity of a few km s^{-1} and a tilt angle of 20° with respect to the azimuthal plane (i.e., with a non-zero axial component of the phase velocity). The density variation was phase-correlated with the oscillating electric field and, as a consequence, an enhanced electron axial mobility was caused. The phase velocity of the rotating spoke was one order of magnitude smaller than the local $\mathbf{E}\times\mathbf{B}$ drift. Moreover, as part of the research, different propellants were used and it turned out that the phase velocity of the spoke scaled with the ionization potential of the neutral gas: xenon, krypton, or argon. All these facts seem to indicate a close connection between the ionization process and the appearance of the spoke. Janes and Lowder made as well use of the statistical theory of Yoshikawa and Rose[13] obtaining a good agreement with the experiments in terms of predicted anomalous diffusion.

Esipchuk *et al.*[22] also reported low frequency azimuthal oscillations in a Hall thruster in the low voltage part of the I–V curve and rotating in the $\mathbf{E}\times\mathbf{B}$ direction. The oscillations for density and electric field were correlated causing enhanced electron conductivity. However, these oscillations disappeared at higher voltage. Based on that, Esipchuk *et al.* claimed this oscillation is due to incomplete ionization in the low-voltage part of the I–V curve and hence disappears in the current saturated part of the curve.

Shortly after, Lomas and Kilkenny[19] reproduced the Janes-Lowder experimental results and carried out an analysis of the influence of the magnetic field. According to the analysis of Lomas and Kilkenny, the phase speed of the spoke increases with the magnetic field, an interesting property not previously described by Janes and Lowder.

During the last two decades, several experiments have been carried out with modern HETs to characterize the low frequency azimuthal oscillations for a wide range of operating conditions and thrusters, both inside and outside the channel. Next is a summary of these studies.

In one of the first of those analyses, Hargus *et al.*[23] study the azimuthal oscillations in a laboratory Hall thruster. The conclusions from that study can be summarized as follows. First, low frequency azimuthal waves are observed at velocities of a few km s^{-1} both in the low-ionization part and the current saturation part of the I–V curve. In the current saturation part of the I–V curve, the wave is closer to the channel exit. In the ionization part of the I–V curve, near the knee, the wave has a lower frequency and is stronger and more spread throughout the thruster. Finally, at very low voltages, the wave is located only near the anode and the wave frequency is higher than in all previous cases.

Meezan and Cappelli[6–8] use several low-frequency diagnosis methods to measure experimentally the electron mobility along the thruster. The results are in line with the general properties of anomalous diffusion presented above, and in particular, with the presence of a dip in the electron conductivity around the region of maximum electron shear. And what is more important, the electron mobility profile computed with the theory of Yoshikawa and Rose[13] from the measured density oscillations matches fairly well the measured electron mobility for various operating conditions. A possible correlation between the dip in the electron conductivity and the electron shear is suggested by Cappelli,[8] although no definitive conclusions have been reached to this respect. A similar mechanism of electron transport barrier due to high electron shear has been proposed in the area of nuclear fusion inside tokamaks,[24] although Hall and nuclear fusion plasmas are in rather different conditions to establish a link between them without a more detailed analysis.

In a separate study, Chesta *et al.*[20] focus on the characterization of all low frequency oscillations in HETs, both axial and azimuthal. In that work, the usual breathing mode and transit time oscillations are clearly observable together with some special azimuthal oscillations. The latter ones are caused first by the azimuthal asymmetry of the magnetic field, generated by four magnetic coils, and second by the presence of two azimuthally separated Langmuir probes. Apart from those oscillations, two additional azimuthal low frequency waves with a tilt angle of 15°–20° and a wave mode number $m = 1$ are detected at low and at high voltage. The oscillation at low voltage has a phase velocity of a few km s^{-1} with a frequency of 5–10 kHz and seems to match the properties of the rotating spoke detected by Janes and Lowder,[14] Esipchuk *et al.*,[22] and Lomas and Kilkenny.[19] On the other hand, the oscillation at high voltage has a frequency of roughly 20 kHz and could be the natural extension of the rotating spoke to the current saturation part of the I–V curve. Moreover, the relative size of the low frequency density oscillations with respect to the azimuthally averaged density shows a dip in most operating conditions around the region of high magnetic field, in agreement with the results of Meezan and Cappelli.[6–8]

Gascon *et al.*[25–27] study the propagation properties of low frequency azimuthal oscillations and analyse the influence of the ceramic material used, either alumina or boron nitride. In that study, gradient-induced azimuthal oscillations are detected at various axial locations in the medium frequency range (30–200 kHz). As in previous studies, azimuthal waves are suppressed around the region of maximum magnetic field. The main novelty of that study is the dependence of the direction of propagation of the azimuthal waves on the ceramic material used. The type of material affects the azimuthal oscillations by controlling the relative position of the magnetic field and plasma density maxima via the secondary electron emission yield of the material. Apart from these medium frequency oscillations, Gascon *et al.* also observe azimuthal oscillations below 30 kHz rotating along $\mathbf{E} \times \mathbf{B}$ in the near anode region, but in the opposite direction in the near-plume.

Smith and Cappelli[28] analyse low frequency oscillations of density, temperature, and electric field in the near field plume of a HET operating in nominal conditions. A density oscillation is detected at the thruster exit that rotates in the $-\mathbf{E} \times \mathbf{B}$ direction with a phase velocity of 1.8 km s^{-1} and a frequency of 25 kHz. The propagation properties of this oscillation agree well with the results previously described, except for the propagation direction which is reported to be opposite to the usual $\mathbf{E} \times \mathbf{B}$ drift. A similar behaviour is reported by Gascon and Cappelli[26] in the outer region of a Hall thruster with alumina as ceramic material.

More recently, Raitses *et al.*[29] have observed spokes in a cylindrical Hall thruster. In a series of experimental studies,[21,30–33] this oscillation is characterized through the use of a segmented anode and high-speed imaging. In this case, the spoke travels in the $+\mathbf{E} \times \mathbf{B}$ direction with a phase speed of about 2 km s^{-1} and an azimuthal wave length of the order of the circumference of the channel, this is, with a wave mode $m = 1$. These properties agree well with other experiments described above. Additionally, the influence of the cathode operation on the spoke and the electron mobility is analysed in that research. In particular, if the cathode emission is increased, the spoke disappears and the electron conductivity is greatly reduced. This is a good indication of the connection between the anomalous diffusion and the spoke oscillation. As a continuation of those analyses, Refs. 34 and 35 show how it is possible to control, suppress, or even promote spoke oscillations by means of a feedback-loop control on the discharge voltage of the elements of a segmented anode.

In a parallel and independent research, McDonald *et al.*[36–38] have used also high-speed imaging techniques as well as a segmented anode to characterize the spoke in a wide range of HETs, including both conventional and non-conventional designs (the H6 thruster, the NASA 173Mv1, the Busek BHT-600, the X2 dual nested channel Hall thruster, and the Helicon Hall thruster). In those analyses, the larger the thruster is, the larger the mode number of the spoke is. In particular, for the H6 thruster modes $m = 2$ and $m = 3$ dominate in nominal operating conditions, whereas $m = 4$ and $m = 5$ are observed to be dominant when using the segmented anode.[36] Another result from that research is that azimuthal oscillations are also found in the near plume of the thruster rotating in the same direction with a similar frequency.[39]

Similarly, Liu[40,41] also finds azimuthal oscillations in the BHT-200 and BHT-600 thrusters via high speed-imaging techniques. Although azimuthal plasma structures are found both at low and high voltages, this is, in the ionization and current saturation parts of the I–V curve, they are more visible at low voltage. Liu finds that the velocity and frequency of the wave increase with the discharge voltage by carrying out several parametric variations. Additionally, Liu also uses krypton as propellant finding similar properties for the spoke oscillation, being the frequency and velocity of the wave higher than with xenon for similar operating conditions.

As conclusion from all these experiments, it can be stated that in modern Hall thrusters the spoke oscillation is an inherent feature of the thruster operation and appears in the ionization and the current saturation parts of the I–V curve, being more pronounced at low voltages.

B. Numerical simulations

Lomas and Kilkenny[19] support their experimental results with the numerical solution of a simplified version of the two-dimensional fluid equations of electrons, ions, and neutrals in a Hall accelerator with hydrogen as propellant. Even though the conditions of the simulations are far from modern HETs, it is interesting to see that low frequency azimuthal oscillations can be promoted by the ionization in a Hall device.

More recently, Lam *et al.*[42] have developed a hybrid code that is the natural extension of Fife's hybrid model[18,43] to the axial-azimuthal space. Azimuthal effects are kept in the formulation at the expense of not solving the radial direction. The results of this code for the nominal operating point of the simulated thruster show a tilted wave with a phase velocity of 4 km s^{-1}, a mode number $m = 4$, and a frequency of

40 kHz. This wave propagates inside the channel in the $\mathbf{E}\times\mathbf{B}$ direction and upstream whereas in the plume the axial direction of propagation of the wave is reversed. This seems to be correlated with the change in the gradient of the magnetic field. Moreover, in the region of maximum magnetic field, the waves are mostly longitudinal as detected experimentally.[26,27]

C. Theory: Low-frequency local-linear-stability models

Most of the stability analyses of the Hall discharge carried out so far are local as opposed to those where the stability is analysed globally. The few studies that do account globally for the axial variations of the inhomogeneous plasma are focused on the high frequency range.[44–48] The local stability analyses covering the low and medium frequency ranges may be grouped according to whether or not they include ionization in the formulation. Let us start our discussion with those that do not take it into account.

Even though there exist previous local stability analyses dedicated to Hall devices,[49,50] Morozov *et al.*[12] carried out the first azimuthal stability analysis of the Hall discharge. They used a cold, two-fluid, quasineutral, collisionless, electrostatic formulation without electron inertia. Their main conclusion was the existence of unstable azimuthal oscillations in regions where the gradient of the magnetic field to plasma density ratio is negative, i.e.,

$$d/dx(B_0/n_0) < 0.$$

Esipchuk and Tilinin[51] extended the linear stability analysis of Morozov *et al.* by accounting for electron inertia, and electromagnetic and non-quasineutral effects. In the electrostatic low frequency and quasineutral limit of the resulting dispersion relation, similar results to those of Morozov[12] were obtained. The stability criterion derived by Esipshuk and Tilinin seems to cover the gradient-induced oscillations measured experimentally in the medium frequency range. Additionally, low frequency quasi-longitudinal waves are predicted when $d/dx(B_0/n_0) > 0$. Furthermore, when electron inertia terms are retained in the model, high frequency, azimuthal, long wavelength oscillations are predicted near the lower-hybrid frequency.

Kapulkin and Guelman[52,53] carry out another stability analysis with a two-fluid formulation specifically suited for the region very close to the anode where the ionization is negligible and the temperature and the magnetic curvature contribute to the azimuthal drift of the electron flow. The main novelty with respect to the work of Esipchuk and Tilinin is the inclusion of electron pressure effects. The electron temperature is included in the model although its oscillations are neglected. The results indicate the presence of an unstable oblique wave of low frequency that can promote electron conductivity towards the anode.

More recently, Frias *et al.*[54,55] have revisited the local stability of the Hall discharge by means of a two-fluid collision-less model and applied the resulting stability criterion to experimental and numerical profiles of the Hall discharge.[56] The local stability analysis of Frias *et al.*[54] resembles those by Morozov *et al.*,[12] and Esipchuk and Tilinin.[51] However, the effect of the compressibility of the electron flow, which includes the $\mathbf{E}\times\mathbf{B}$ and the diamagnetic drifts, is accounted for completely, yielding a stability criterion with different numerical factors, but qualitatively similar in form to those obtained by Morozov *et al.* and by Esipchuk and Tilinin. Additionally, the effect of the electron temperature oscillations on the stability is evaluated by Frias *et al.* The resulting stability criterion shows similar features to the analysis without electron temperature oscillations, but near the stability threshold, the differences are important, causing that stable cases in the simplified model become unstable if electron temperature perturbations are accounted for. However, no attempt is done to analyse the influence of the ionization in the stability of the discharge in the low-frequency range.

Within the group of local stability analyses accounting for ionization, the first work is due to Lomas and Kilkenny[19] in the 1970s. Beyond reproducing the Janes-Lowder experimental results and using numerical simulations to analyze the spoke oscillation, they carried out a linear stability analysis of the Hall accelerator and suggested that the spokes detected experimentally are linked to the growth of electrothermal instabilities. However, the analysis is performed for hydrogen, instead of a more typical propellant of modern Hall thrusters like xenon.

Chesta *et al.*[57] evaluate numerically the linear stability of experimental steady-state profiles with a three-fluid description of the discharge including ionization, particle collisions, and electromagnetic effects. The main conclusion of that research is that low frequency azimuthal oscillations are largely caused by the ionization process and driven in part by the gradients of the magnetic field and plasma density. However, no investigation is carried out to describe the exact mechanism of the instability by means of simple analytical expressions.

Gallardo and Ahedo[58] use a three-fluid formalism without electromagnetic terms to analyse the relation of the low frequency azimuthal waves with the electron anomalous diffusion. The main novelty with respect to previous studies is that the azimuthal three-fluid unsteady equations are solved to observe non-linear saturation effects. The conditions analysed in that case correspond to the ionization region of the channel. The results predict an $m=3$ azimuthal wave promoted by the ionization process with a phase velocity of 2.7 km s^{-1} travelling in the $-\mathbf{E}\times\mathbf{B}$ direction.

Finally, Malik and Singh[59] perform a local stability analysis accounting for ionization partially. The ion and electron equations do contain source terms related to ionization, but the model does not include the neutral equations, which are important in the low frequency range. In fact, the breathing mode, one of the main low frequency longitudinal oscillations in Hall thrusters, cannot be reproduced without considering the neutrals as part of the model. The results from Malik and Singh predict unstable oscillations in the range of 100 kHz, which is above the range where the spoke is normally measured.

As a conclusion from this literature review, it can be stated that it is worth to revisit the local linear stability of the Hall discharge accounting for the ionization process completely, that is, with the conservation equations of the neutral species. This is the topic of Sec. III.

III. AZIMUTHAL LINEAR STABILITY ANALYSES OF THE IONIZATION REGION

As shown in the previous section, there is experimental evidence of low frequency azimuthal oscillations in the ionization region of the HET discharge. In this region, the ionization plays a major role in the definition of the axial profile of the main plasma variables. In order to account for this process in a stability analysis, a three-fluid model (ions, electrons, and neutrals) needs to be considered. This section presents results from two separate models: a simple one, where the temperature is considered uniform and without oscillations; and a more complete one, that includes an electron energy equation and heat conduction terms in order to account for temperature gradients and oscillations.

Both models are based on a formulation consisting of particle, momentum, and energy conservation equations for electrons, ions, and neutrals separately

$$\frac{\partial n}{\partial t}+\nabla\cdot(n\mathbf{v}_e)=nn_n\xi_{ion}, \tag{1}$$

$$\frac{\partial n}{\partial t}+\nabla\cdot(n\mathbf{v}_i)=nn_n\xi_{ion}, \tag{2}$$

$$\frac{\partial n_n}{\partial t}+\nabla\cdot(n_n\mathbf{v}_n)=-nn_n\xi_{ion}, \tag{3}$$

$$0=\nabla(nT_e)+en(\mathbf{E}+\mathbf{v}_e\times\mathbf{B})+m_enn_n\xi_e\mathbf{v}_e, \tag{4}$$

$$m_in\left(\frac{\partial\mathbf{v}_i}{\partial t}+\mathbf{v}_i\cdot\nabla\mathbf{v}_i\right)=en\mathbf{E}-m_inn_n\xi_{ion}(\mathbf{v}_i-\mathbf{v}_n), \tag{5}$$

$$m_nn_n\left(\frac{\partial\mathbf{v}_n}{\partial t}+\mathbf{v}_n\cdot\nabla\mathbf{v}_n\right)=\mathbf{0}, \tag{6}$$

$$\frac{\partial}{\partial t}\left(\frac{3}{2}nT_e\right)+\nabla\cdot\left(\frac{5}{2}nT_e\mathbf{v}_e+\mathbf{q}_e\right)=-en\mathbf{v}_e\cdot\mathbf{E}-nn_n\xi_{ion}E'_{ion}, \tag{7}$$

$$\frac{5}{2}nT_e\nabla T_e+e\mathbf{q}_e\times\mathbf{B}+m_en_n\xi_e\mathbf{q}_e=\mathbf{0}, \tag{8}$$

where $_{i,e,n}$ are the sub-indexes for ion, electron, and neutral species; e is the electron charge; m_e, m_i, and m_n are the electron, ion, and neutral masses; $\mathbf{E}$ and $\mathbf{B}$ are the electric and magnetic fields; n and n_n are plasma and neutral densities; $\mathbf{v}_j$ is the velocity vector of species j; ξ_{ion} and ξ_e are the ionization and the effective electron collision rates; T_e is electron temperature; E'_{ion} is the energy loss per effective single ionization event; and $\mathbf{q}_e$ is the electron heat conduction flux vector. The quasi-neutrality assumption ($n_e=n_i$) has been used in the formulation since the Debye length is much smaller than the typical dimensions of the thruster. Finally, notice as well that the induced magnetic field is neglected and thus, the electric field derives from an electric potential, ϕ ($\nabla\phi=-\mathbf{E}$), and the magnetic field is equal to the externally applied field, resulting in an electrostatic formulation.

A. Isothermal model

In this case, electron temperature gradients and oscillations are neglected in the formulation, and therefore, Eqs. (7) and (8) are not used. The corresponding steady state ($\partial/\partial t=0$) zero-th order solution (expressed with subindex 0) is considered azimuthally symmetric ($\partial/\partial y=0$). The zero-th order solution then verifies

$$\frac{dn_{n0}}{dx}=-\frac{n_0n_{n0}\xi_{ion0}}{v_{nx0}}, \tag{9}$$

$$\frac{dv_{nx0}}{dx}=0, \tag{10}$$

$$\frac{dv_{ix0}}{dx}=n_{n0}\xi_{ion0}-v_{ix0}\frac{d\ln n_0}{dx}, \tag{11}$$

$$\frac{e}{m_i}E_0=v_{ix0}\frac{dv_{ix0}}{dx}+n_{n0}\xi_{ion0}(v_{ix0}-v_{nx0}), \tag{12}$$

$$\frac{dv_{ex0}}{dx}=n_{n0}\xi_{ion0}-v_{ex0}\frac{d\ln n_0}{dx}, \tag{13}$$

$$v_{ex0}=v_{ey0}\frac{\nu_{e0}}{\omega_{ce}}, \tag{14}$$

$$v_{ey0}=-\frac{1}{B_0}\left(E_0+\frac{T_{e0}}{e}\frac{d\ln n_0}{dx}\right), \tag{15}$$

where ω_{ce} is the electron cyclotron frequency, $\nu_{e0}=n_{n0}\xi_{e0}$ is the effective electron collision frequency, and the Hall parameter is assumed to be very large ($\omega_{ce}/\nu_{e0}\gg1$).

As shown by Ahedo *et al.* in Ref. 16, the solution of Eqs. (9)–(15) together with the proper boundary conditions verifies the following properties. The axial electron velocity is negative all along the thruster channel as electrons drift from the cathode to the anode. On the contrary, the neutral axial velocity is positive as the gas moves from the injector to the channel exit. In the case of the axial ion velocity, it is positive in a large part of the thruster channel due to the electric acceleration ($E_0>0$), but it becomes negative in an ion back-streaming region near the anode where the axial electric field is mildly negative and attracts the ions to the anode ($E_0<0$). The azimuthal electron velocity is also negative all along the thruster and consists of the $\mathbf{E}\times\mathbf{B}$ and the diamagnetic drifts, being the $\mathbf{E}\times\mathbf{B}$ drift the dominant one in the acceleration region, while the diamagnetic drift dominates in the upstream part of the ionization region. As for the plasma density gradient, it is positive from the anode to the beginning of the acceleration region, from where it becomes negative as a consequence of the ion acceleration.

Assuming small perturbations with respect to the zero-th order state ($\hat{f}\ll f_0$), except for T_e which is considered constant, Eqs. (1)–(6) may be linearised into

$$\frac{\partial\hat{n}}{\partial t}+n_0\left(\frac{\partial\hat{v}_{ex}}{\partial x}+\frac{\partial\hat{v}_{ey}}{\partial y}\right)+\hat{v}_{ex}\frac{dn_0}{dx}+v_{ex0}\frac{\partial\hat{n}}{\partial x}+v_{ey0}\frac{\partial\hat{n}}{\partial y}+\hat{n}\frac{dv_{ex0}}{dx}=(n_0\hat{n}_n+\hat{n}n_{n0})\xi_{ion0}, \tag{16}$$

$$\frac{\partial\hat{n}}{\partial t}+n_0\left(\frac{\partial\hat{v}_{ix}}{\partial x}+\frac{\partial\hat{v}_{iy}}{\partial y}\right)+\hat{v}_{ix}\frac{dn_0}{dx}+v_{ix0}\frac{\partial\hat{n}}{\partial x}+\hat{n}\frac{dv_{ix0}}{dx}=(n_0\hat{n}_n+\hat{n}n_{n0})\xi_{ion0}, \tag{17}$$

$$\frac{\partial\hat{n}_n}{\partial t}+n_{n0}\left(\frac{\partial\hat{v}_{nx}}{\partial x}+\frac{\partial\hat{v}_{ny}}{\partial y}\right)+\hat{v}_{nx}\frac{dn_{n0}}{dx}+v_{nx0}\frac{\partial\hat{n}_n}{\partial x}=-(n_0\hat{n}_n+\hat{n}n_{n0})\xi_{ion0}, \tag{18}$$

$$0 = -\frac{1}{n_0}\frac{T_{e0}}{m_e}\frac{\partial \hat{n}}{\partial x} + \frac{\hat{n}}{n_0^2}\frac{T_{e0}}{m_e}\frac{dn_0}{dx} + \frac{e}{m_e}\left(\frac{\partial \hat{\phi}}{\partial x} - \hat{v}_{ey}B_0\right) - (n_{n0}\hat{v}_{ex} + \hat{n}_n v_{ex0})\xi_{e0}, \tag{19}$$

$$0 = -\frac{1}{n_0}\frac{T_{e0}}{m_e}\frac{\partial \hat{n}}{\partial y} + \frac{e}{m_e}\left(\frac{\partial \hat{\phi}}{\partial y} + \hat{v}_{ex}B_0\right) - (n_{n0}\hat{v}_{ey} + \hat{n}_n v_{ey0})\xi_{e0}, \tag{20}$$

$$\frac{\partial \hat{v}_{ix}}{\partial t} + v_{ix0}\frac{\partial \hat{v}_{ix}}{\partial x} + \hat{v}_{ix}\frac{dv_{ix0}}{dx} = -\frac{e}{m_i}\frac{\partial \hat{\phi}}{\partial x} - n_{n0}\xi_{ion0}(\hat{v}_{ix} - \hat{v}_{nx}) - \hat{n}_n\xi_{ion0}(v_{ix0} - v_{nx0}), \tag{21}$$

$$\frac{\partial \hat{v}_{iy}}{\partial t} + v_{ix0}\frac{\partial \hat{v}_{iy}}{\partial x} = -\frac{e}{m_i}\frac{\partial \hat{\phi}}{\partial y} - n_{n0}\xi_{ion0}(\hat{v}_{iy} - \hat{v}_{ny}), \tag{22}$$

$$\frac{\partial \hat{v}_{nx}}{\partial t} + v_{nx0}\frac{\partial \hat{v}_{nx}}{\partial x} = 0, \tag{23}$$

$$\frac{\partial \hat{v}_{ny}}{\partial t} + v_{nx0}\frac{\partial \hat{v}_{ny}}{\partial x} = 0, \tag{24}$$

where it is assumed that the collision and ionization rates are constant ($\xi_e = \xi_{e0}$, $\xi_{ion} = \xi_{ion0}$).

The perturbations may be assumed to be of the following Fourier form:

$$\hat{f}(t,x,y) = \bar{f}(x)\exp(-i\omega t + ik_y y), \tag{25}$$

where t is the time variable, x and y are the axial and azimuthal coordinates in the quasi-planar approximation, $\bar{f}(x)$ is the x-dependent coefficient of the Fourier-expanded perturbation of a generic variable f, and ω and k_y are the angular frequency and azimuthal wave number, respectively. Note that the y axis is along the $-\mathbf{E}\times\mathbf{B}$ direction and that k_y may only take a discrete number of values given the azimuthal symmetry of the problem. This type of Fourier expansion is the basis of global stability studies, where the resulting formulation is not algebraic, but consists of differential equations. Within the linear regime, that global approach is fully consistent for inhomogeneous plasmas as opposed to the local analysis carried out here.

As part of the current local analysis, the axial variation of the perturbations is also Fourier-expanded resulting in

$$\hat{f}(t,x,y) = \bar{f}\exp(ik_x x)\exp(-i\omega t + ik_y y), \tag{26}$$

where k_x is the axial wave number and $\bar{f}$ is the coefficient of the Fourier-expanded perturbation. The tilt angle of the oscillation may be then expressed as $\arctan(k_x/k_y)$.

In this local analysis, it is necessary to freeze the zero-th order variables and their gradients and consider them constant, even if in reality the plasma is inhomogeneous along x, so that the Fourier expansion in the x direction can be carried out. This is supported by the assumption that the length scale of the axial variation of the zero-th order variables (L_x) is much larger than the axial wave-length of the perturbations ($k_x L_x \gg 1$). This is the so-called Boussinesque approximation[54] and allows reducing the formulation to an algebraic problem. In Hall thrusters, this condition is not strictly met and thus the solutions from local stability analyses must be considered as an approximate limiting case. In fact, some authors claim that depending on how the equations are linearised and Fourier-expanded as part of the local stability analysis, the resulting stability criterion may change.[60] In any case, the local analysis does provide some insights into the stability of the Hall discharge and is an important step to take before analysing the linear stability with a global approach.

Equations (16)–(24) contain four gradients of zero-th order variables (dn_0/dx, dn_{n0}/dx, dv_{ix0}/dx, dv_{ex0}/dx). Making use of Eqs. (9)–(15) and the length scale of the axial variation of the plasma density, l_n:

$$l_n = (d\ln n_0/dx)^{-1} \tag{27}$$

those four gradients may be expressed as a function only of the zeroth order variables and l_n. It is important to note that the gradient of the magnetic field does not appear in the formulation as the expressions for the axial and azimuthal electron velocities in Eqs. (14) and (15) have been linearised and Fourier expanded rather than introduced in the rest of expressions in Eqs. (9)–(13) before the linearisation, as Esipchuk and Tilinin[51] and Frias *et al.*[54] do. The consequences of this choice are discussed in Ref. 60 and evaluated in the next section.

Additionally, it is possible to make the problem non-dimensional by defining the following reference variables for mass, charge, time, density, and length, respectively: m_i, e, Ω^{-1}, n_0, and L, where Ω and L are arbitrary reference values here assumed to be, respectively, 10 kHz and 1 cm. Hereinafter, non-dimensional variables are expressed with a tilde above the variable symbol. For instance, $\tilde{l}_n = l_n/L$ represents the non-dimensional length scale of the axial variation of plasma density.

The non-dimensional Fourier form of the linearised equations may be written as an eigenvalue problem in matrix form as

$$(A\tilde{\omega} + B)\tilde{\mathbf{w}} = \mathbf{0}, \tag{28}$$

where $\tilde{\mathbf{w}} = (\tilde{n}, \tilde{n}_n, \tilde{v}_{ix}, \tilde{v}_{iy}, \tilde{\phi}, \tilde{v}_{ex}, \tilde{v}_{ey})$ is the vector of non-dimensional variables, A and B are matrices of size 7×7, which are functions of the vector of non-dimensional parameters defining the zero-th order solution, $\tilde{\mathbf{p}}_0 = (\tilde{n}_{n0}, \tilde{v}_{ix0}, \tilde{v}_{nx0}, \tilde{\xi}_{ion0}, \tilde{\xi}_{e0}, \tilde{T}_{e0}, \tilde{B}_0)$, and the non-dimensional wave-numbers in the axial and azimuthal directions, $\tilde{k}_x$ and $\tilde{k}_y$. Equation (28) constitutes an eigenvalue problem with one unknown, the *complex* oscillation frequency, $\tilde{\omega} = \tilde{\omega}_{re} + i\tilde{\omega}_{im}$, as function of the wave numbers and the vector of parameters, this is, $\tilde{\omega}(\tilde{k}_x, \tilde{k}_y, \tilde{\mathbf{p}}_0)$. Since the electron inertia and electromagnetic and non-quasineutral terms have been neglected, no time derivatives of $\tilde{v}_{ex}$, $\tilde{v}_{ey}$, and $\tilde{\phi}$ appear in the formulation. Thanks to this, three equations may be pre-eliminated in the matrix formulation and there remain only four solutions for $\tilde{\omega}$ in Eq. (28).

In the remainder of the analysis, we will focus on purely azimuthal oscillations ($\tilde{k}_x = 0$) in an attempt to reproduce and analyse the spoke oscillations. Notice that under that condition, the perturbations of the axial and azimuthal neutral velocity are zero ($\tilde{v}_{nx} = \tilde{v}_{ny} = 0$) according to the

perturbed neutral momentum equations. Moreover, we will study the limited region of the thruster channel where $dn_0/dx > 0$ and $dv_{ix0}/dx > 0$ due to ionization and a positive zero-th order electric field ($E_0 > 0$).

1. Approximate solution

Let us first consider a particular case, where an analytical solution for the dispersion relation can be found. This consists of the collisionless case ($\tilde{\xi}_{e0} = 0$) at the particular cross-section where $\tilde{v}_{nx0} = \tilde{v}_{ix0}$, located inside the ionization region. Then, the dispersion relation in Eq. (28) simplifies into

$$0 = (\tilde{\omega} + i\tilde{n}_{n0}\tilde{\xi}_{ion0})\left((\tilde{\omega} - i\tilde{v}_{ix0}/\tilde{l}_n) - \frac{\tilde{n}_{n0}\tilde{\xi}^2_{ion0}}{\tilde{\omega} + i\tilde{\xi}_{ion0}}\right) + \tilde{k}_y\tilde{l}_n\tilde{B}_0\left(\tilde{\omega} - \tilde{k}_y(\tilde{T}_{e0}/\tilde{l}_n - \tilde{E}_0)/\tilde{B}_0 - \frac{\tilde{n}_{n0}\tilde{\xi}^2_{ion0}}{\tilde{\omega} + i\tilde{\xi}_{ion0}}\right). \tag{29}$$

Equation (29) is cubic in $\tilde{\omega}$ and thus has three solutions. The fourth solution of Eq. (28), not captured in Eq. (29), comes from Eq. (21) and is stable ($\tilde{\omega}_{re} > 0$) under the current assumptions.

For typical conditions in the ionization region of a Hall thruster, it holds approximately that $\tilde{n}_{n0} \gg 1$, $\tilde{\xi}_{ion0} \ll 1$, $\tilde{n}_{n0}\tilde{\xi}_{ion0} \sim 1$, and $\tilde{v}_{ix0} \sim 1$. Taking into account those orders of magnitude, Eq. (29) simplifies into the following second order equation:

$$0 = \tilde{\omega}^2 + \tilde{\omega}(i\tilde{n}_{n0}\tilde{\xi}_{ion0} - i\tilde{v}_{ix0}/\tilde{l}_n + \tilde{k}_y\tilde{l}_n\tilde{B}_0) + \tilde{n}_{n0}\tilde{\xi}_{ion0}\tilde{v}_{ix0}/\tilde{l}_n - \tilde{k}_y^2\tilde{l}_n(\tilde{T}_{e0}/\tilde{l}_n - \tilde{E}_0) \tag{30}$$

plus the marginally stable solution $\tilde{\omega} \approx -i\tilde{\xi}_{ion0}$. The solutions of Eq. (30) are in the low frequency range, and are unstable ($\tilde{\omega}_{im} > 0$) when

$$(\tilde{k}_y\tilde{l}_n)^2 < \frac{\tilde{n}_{n0}\tilde{\xi}_{ion0}\tilde{v}_{ix0}}{\tilde{T}_{e0}/\tilde{l}_n - \tilde{E}_0}, \tag{31}$$

where the evaluation is performed in the near anode region, where the electron pressure gradient, $\tilde{T}_{e0}/\tilde{l}_n$, dominates over the electric field, $\tilde{E}_0$, and hence the denominator of the expression (31) is positive. According to Eq. (30), the highest growth rate is obtained for the perturbation with the smallest wave number allowed by the azimuthal continuity condition, which imposes a lower limit on the azimuthal wave number. Note as well that the most unstable solution of Eq. (30) verifies that the product of $\tilde{\omega}_{re}$ and $\tilde{k}_y$ is negative, indicating that the wave propagates in the $-y$ direction, that is, along $+\mathbf{E}\times\mathbf{B}$.

2. Full numerical solution

The numerical solution of the isothermal model in Eq. (28) is discussed in this subsection. To this end, several parametric analyses are presented in this section with respect to different parameters ($\tilde{v}_{nx0}$, $\tilde{n}_{n0}$, $\tilde{T}_{e0}$, $\tilde{\xi}_{ion0}$, and $\tilde{B}_0$) together with the azimuthal wave number, $\tilde{k}_y$. In all of them, it is possible to observe unstable solutions for low wave numbers in agreement with the particular analysis in the previous subsection.

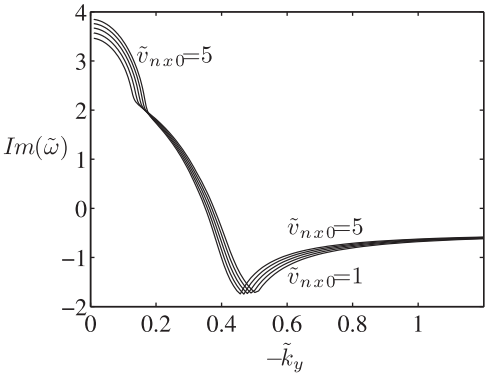

FIG. 1. Growth rate of the most unstable solution of Eqs. (16)–(24) for the following non-dimensional parameters: $\tilde{n}_{n0} = 20$, $\tilde{v}_{ix0} = 5$, $\tilde{\xi}_{ion0} = 0.5$, $\tilde{\xi}_{e0} = 0$, $\tilde{T}_{e0} = 450$ and $\tilde{B}_0 = 1$. Parametric variation of $\tilde{k}_y$ and $\tilde{v}_{nx0}$.

For the resolution of Eq. (28), the following typical values for the macroscopic variables in the ionization region of a HET are used: neutral velocity at injection, $v_{nx0} = 500\,\mathrm{m\ s^{-1}}$; neutral density, $n_{n0} = 10^{19}\,\mathrm{m^{-3}}$; electron temperature, $T_{e0} = 6\,\mathrm{eV}$; ionization frequency, $\nu_{i0} = n_{n0}\xi_{ion0} = 10^5\,\mathrm{Hz}$; and magnetic field, $B_0 = 140$ G. Additionally, the following values for the reference parameters are used: $m_i = 2.2\times10^{-25}$ kg, $e = 1.6\times10^{-19}$ C, $\Omega = 10\,\mathrm{kHz}$, $n_0 = 5\times10^{17}\,\mathrm{m^{-3}}$, and $L = l_n = 1$ cm. The resulting non-dimensional variables are $\tilde{v}_{nx0} = 5$, $\tilde{n}_{n0} = 20$, $\tilde{T}_{e0} = 450$, $\tilde{\xi}_{ion0} = 0.5$, $\tilde{l}_n = 1$, and $\tilde{B}_0 = 1$. These parameters define the reference state with respect to which the parametric variations are carried out below. It is also interesting to point out that under these conditions a non-dimensional value of the wave number of $\tilde{k}_y = -0.25$ is equivalent to an oscillation travelling in the $+\mathbf{E}\times\mathbf{B}$ direction with a wavelength of around 24 cm, which is the same as the perimeter of a circumference with a mean radius of 4 cm, a typical value for a modern HET. Thus, $\tilde{k}_y = -0.25$ corresponds to a mode $m = 1$ and wave numbers below that threshold are not possible due to azimuthal continuity.

Figure 1 shows the influence of the neutral velocity on the growth rate of the perturbations. Note that one of the cases plotted is the one studied analytically previously, $\tilde{v}_{nx0} = \tilde{v}_{ix0}$. Figure 2 shows the growth rate as a function of

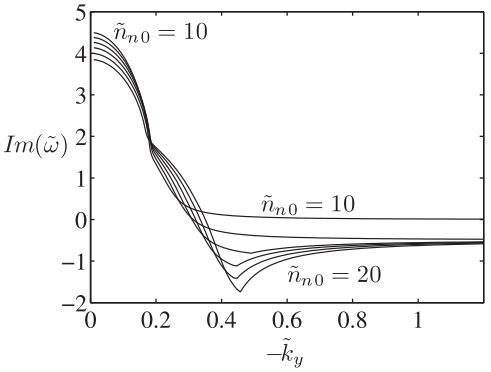

FIG. 2. Growth rate of the most unstable solution of Eqs. (16)–(24) for the following non-dimensional parameters: $\tilde{v}_{ix0} = 5$, $\tilde{v}_{nx0} = 5$, $\tilde{\xi}_{ion0} = 0.5$, $\tilde{\xi}_{e0} = 0$, $\tilde{T}_{e0} = 450$ and $\tilde{B}_0 = 1$. Parametric variation of $\tilde{k}_y$ and $\tilde{n}_{n0}$.

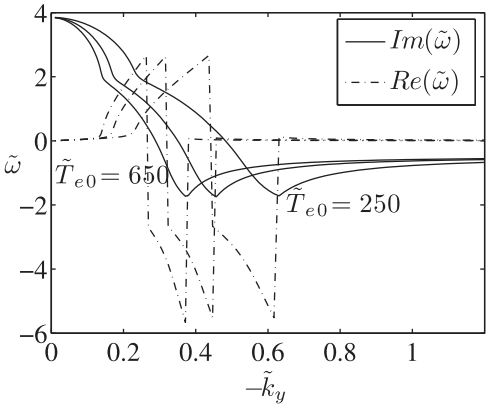

FIG. 3. Growth rate (-) and real part (··) of the most unstable solution of Eqs. (16)–(24) for the following non-dimensional parameters: $\tilde{n}_{n0}=20$, $\tilde{v}_{ix0}=5$, $\tilde{v}_{nx0}=5$, $\tilde{\xi}_{ion0}=0.5$, $\tilde{\xi}_{e0}=0$ and $\tilde{B}_0=1$. Parametric variation of $\tilde{k}_y$ and $\tilde{T}_{e0}$.

$\tilde{k}_y$ and $\tilde{n}_{n0}$. The smaller the neutral density is, the smaller the range of wave numbers for unstable perturbations. Fig. 3 shows both the growth rate and the frequency of the oscillation as a function of $\tilde{k}_y$ and $\tilde{T}_{e0}$. As the electron temperature increases, the range of wave numbers for unstable solutions is reduced. In this case, it is also possible to observe that instabilities exist with a frequency around 10 kHz, $\tilde{\omega}_{re}=1$, and a wavelength around 24 cm, $\tilde{k}_y=-0.25$. Note that a frequency of 10 kHz and a wavelength of 24 cm in the $+\mathbf{E}\times\mathbf{B}$ direction correspond to an $m=1$ oscillation with a phase velocity of about 2.4 km s^{-1}, very similar to the ion acoustic speed and to the velocity of the spoke usually measured in experiments.

Figures 4 and 5 show the variation of the growth rate of the most unstable perturbation as a function of $\tilde{k}_y$ and $\tilde{B}_0$ and of $\tilde{k}_y$ and $\tilde{\xi}_{ion0}$, respectively. Fig. 4 shows that the higher the magnetic field, the wider the range of wave numbers for unstable solutions. Moreover, for a given wave number (e.g., $\tilde{k}_y=-0.25$), the frequency of the oscillation increases with the magnetic field. From Fig. 5, it can be stated that the higher the ionization rate, the wider the range for unstable solutions. Moreover, even though the oscillation with the largest growth rate is still the $m=1$ mode, the difference in growth-rate for different wave numbers is greatly reduced when the ionization rate is increased making it possible to

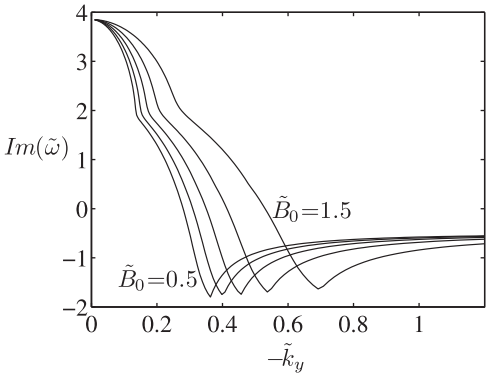

FIG. 4. Growth rate of the most unstable solution of Eqs. (16)–(24) for the following non-dimensional parameters: $\tilde{n}_{n0}=20$, $\tilde{v}_{ix0}=5$, $\tilde{v}_{nx0}=5$, $\tilde{\xi}_{ion0}=0.5$, $\tilde{\xi}_{e0}=0$ and $\tilde{T}_{e0}=450$. Parametric variation of $\tilde{k}_y$ and $\tilde{B}_0$.

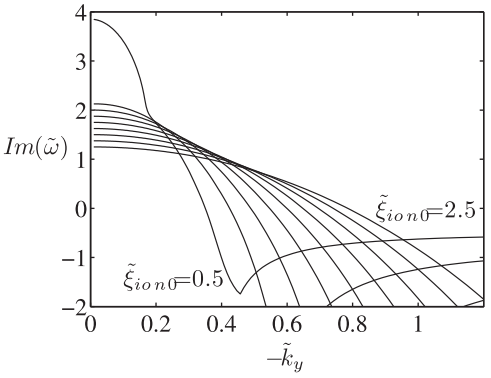

FIG. 5. Growth rate of the most unstable solution of Eqs. (16)–(24) for the following non-dimensional parameters: $\tilde{n}_{n0}=20$, $\tilde{v}_{ix0}=5$, $\tilde{v}_{nx0}=5$, $\tilde{\xi}_{e0}=0$, $\tilde{T}_{e0}=450$ and $\tilde{B}_0=1$. Parametric variation of $\tilde{k}_y$ and $\tilde{\xi}_{ion0}$.

have unstable oscillations with higher wave mode numbers ($m=2$, $m=3\ldots$), as found experimentally.[36] To this respect, while it is true that the model predicts that the $m=1$ mode has the largest unstable growth rate and that other unstable modes $m=2$, $m=3$ and higher exist with lower growth rates, it is also important to note that the current analysis is linear and local and that the final dominant mode can only be fully determined if non-linear effects are accounted for. The relevant result from our analysis is that it is for low wave numbers when the perturbations become unstable, in line with experimental evidence and contrary to the results from the analysis of Frias *et al.*, where the larger the wave number, the larger the growth rate.

Figure 6 depicts a map of the growth rate of the oscillation as a function of the neutral density and the electron temperature for a fixed azimuthal wave number ($\tilde{k}_y=-0.25$). In our model, as the electron temperature is increased and the neutral-to-plasma density ratio is decreased, the growth rate decreases up to the point where the perturbation is no longer unstable. Experiments show that as the discharge voltage is increased, keeping the rest of parameters constant, the intensity of low frequency oscillations diminishes considerably, specially in the ionization part of the I–V curve of the thruster.[61,62] Thus, the linear model is in line with that experimental trend as a discharge voltage increase causes an increase of the electron temperature in the ionization region of the thruster via ohmic heating and a decrease of the neutral-to-plasma density ratio thanks to improved ionization.

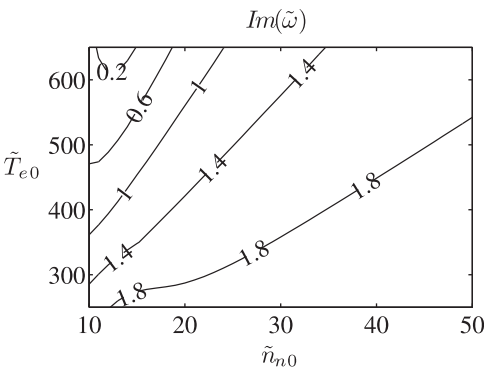

FIG. 6. Growth rate of the most unstable solution of Eqs. (16)–(24) for the following non-dimensional parameters: $\tilde{k}_y=-0.25$, $\tilde{v}_{ix0}=5$, $\tilde{v}_{nx0}=5$, $\tilde{\xi}_{ion0}=0.5$, $\tilde{\xi}_{e0}=0$ and $\tilde{B}_0=1$. Parametric variation of $\tilde{n}_{n0}$ and $\tilde{T}_{e0}$.

3. Simplified model

The dispersion relation in Eq. (30) is equivalent to the following linearised system of perturbation equations in non-dimensional form:

$$\frac{\partial \tilde{\hat{n}}}{\partial \tilde{t}} + \frac{\partial \tilde{\hat{v}}_{ey}}{\partial \tilde{y}} + \frac{\tilde{\hat{v}}_{ex}}{\tilde{l}_n} + \tilde{v}_{ey0}\frac{\partial \tilde{\hat{n}}}{\partial \tilde{y}} = 0, \tag{32}$$

$$\frac{\partial \tilde{\hat{n}}}{\partial \tilde{t}} + \frac{\partial \tilde{\hat{v}}_{iy}}{\partial \tilde{y}} - \tilde{\hat{n}}\frac{\tilde{v}_{ix0}}{\tilde{l}_n} = 0, \tag{33}$$

$$\tilde{\hat{v}}_{ey}\tilde{B}_0 = \tilde{\hat{n}}\tilde{T}_{e0}/\tilde{l}_n, \tag{34}$$

$$0 = \tilde{T}_{e0}\frac{\partial \tilde{\hat{n}}}{\partial \tilde{y}} - \frac{\partial \tilde{\hat{\phi}}}{\partial \tilde{y}} - \tilde{\hat{v}}_{ex}\tilde{B}_0, \tag{35}$$

$$\frac{\partial \tilde{\hat{v}}_{iy}}{\partial \tilde{t}} + \frac{\partial \tilde{\hat{\phi}}}{\partial \tilde{y}} + \tilde{n}_{n0}\tilde{\xi}_{ion0}\tilde{\hat{v}}_{iy} = 0. \tag{36}$$

Notice that the ionization terms are compensated by the gradients of the zero-th order solution in the continuity equations, explaining why there are no source terms in those equations.

If all equations in (32)–(36) are combined into one equation for the non-dimensional plasma density, the result is

$$0 = \frac{\partial^2 \tilde{\hat{n}}}{\partial \tilde{t}^2} - \tilde{l}_n\tilde{B}_0\frac{\partial^2 \tilde{\hat{n}}}{\partial \tilde{t}\partial \tilde{y}} - \tilde{l}_n\left(\frac{\tilde{T}_{e0}}{\tilde{l}_n} - \tilde{E}_0\right)\frac{\partial^2 \tilde{\hat{n}}}{\partial \tilde{y}^2} + \tilde{n}_{n0}\tilde{\xi}_{ion0}\left(\frac{\partial \tilde{\hat{n}}}{\partial \tilde{t}} - \tilde{\hat{n}}\frac{\tilde{v}_{ix0}}{\tilde{l}_n}\right) - \frac{\partial \tilde{\hat{n}}}{\partial \tilde{y}}\frac{\tilde{v}_{ix0}}{\tilde{l}_n}. \tag{37}$$

Since $\tilde{T}_{e0}/\tilde{l}_n - \tilde{E}_0 > 0$, expression (37) is a wave-type equation with a term $(\partial^2\tilde{\hat{n}}/\partial\tilde{y}^2)$ whose coefficient $(-\tilde{c}^2) = -\tilde{l}_n(\tilde{T}_{e0}/\tilde{l}_n - \tilde{E}_0) < 0$ corresponds to a wave velocity, $\tilde{c} = \sqrt{\tilde{T}_{e0} - \tilde{l}_n\tilde{E}_0} \approx \sqrt{\tilde{T}_{e0}}$, of the order of the ion acoustic speed. Moreover, the destabilizing element in Eq. (37) corresponds to the term $\tilde{n}\tilde{n}_{n0}\tilde{\xi}_{ion0}\tilde{v}_{ix0}/\tilde{l}_n$, which is associated to ionization and comes from the coupling between the continuity and momentum equations of the ion species.

However, the solution of the eigenvalue problem associated to Eqs. (32)–(36), that is Eq. (30), indicates that, even though there are unstable perturbations ($\tilde{\omega}_{im} > 0$), the phase speed of the oscillations is very close to zero ($\tilde{\omega}_{re} \approx 0$). The reason for this is that in the previous approximation several terms have been neglected, in particular, the variation of neutral density.

If neutral density oscillations are reintroduced in the previous system, Eqs. (32) and (33) are modified as indicated below and the neutral continuity equation is added to the set of equations

$$\frac{\partial \tilde{\hat{n}}}{\partial \tilde{t}} + \frac{\partial \tilde{\hat{v}}_{ey}}{\partial \tilde{y}} + \frac{\tilde{\hat{v}}_{ex}}{\tilde{l}_n} + \tilde{v}_{ey0}\frac{\partial \tilde{\hat{n}}}{\partial \tilde{y}} = \tilde{\hat{n}}_n\tilde{\xi}_{ion0}, \tag{38}$$

$$\frac{\partial \tilde{\hat{n}}}{\partial \tilde{t}} + \frac{\partial \tilde{\hat{v}}_{iy}}{\partial \tilde{y}} - \tilde{\hat{n}}\frac{\tilde{v}_{ix0}}{\tilde{l}_n} = \tilde{\hat{n}}_n\tilde{\xi}_{ion0}, \tag{39}$$

$$\frac{\partial \tilde{\hat{n}}_n}{\partial \tilde{t}} = -(\tilde{\hat{n}}\tilde{n}_{n0} + \tilde{\hat{n}}_n)\tilde{\xi}_{ion0}. \tag{40}$$

Equations (34)–(36) and (38)–(40), consistent with Eq. (29), represent the minimal system of linear equations capable of reproducing the results from the full solution of the eigenvalue problem given by Eqs. (16)–(24) in terms of phase speed and growth rate of the unstable perturbations for typical HET conditions.

B. Model with energy equation and heat conduction

In the previous section, a simplified stability analysis has been carried out accounting for the ionization process. However, the electron temperature was considered uniform and without oscillations, and consequently, no energy equation was included in the formulation. In this section, both assumptions are relaxed in order to check whether the instability detected with the isothermal model still appears with a more complex model including heat conduction terms. Nevertheless, electron inertia terms and plasma non-quasi-neutrality are still neglected since they are not believed to influence the low frequency instability under analysis.

Under the previous hypothesis, the complete set of governing conservation laws in Eqs. (1)–(8) is considered, including the electron energy conservation equation and the diffusive model for the electron heat conduction flux. In order to close the formulation, a hypothesis about the zero-th order temperature gradient is needed. In this case, an adequate choice seems to be assuming a fixed zero-th order electron temperature axial gradient as suggested by Gallardo and Ahedo.[58] Moreover, the ionization and effective collision rates, ξ_{ion} and ξ_e, are considered constant, neglecting their dependence with the temperature, which is not considered critical for this analysis.

After the linearisation of the equations and the use of a Fourier-like form for the perturbations, the set of equations (16)–(24) is modified and extended with 3 more equations. In particular, the electron momentum equations, (19) and (20), are modified to account for electron temperature oscillations and additionally an electron energy equation and two equations for the electron heat flux vector are added:

$$0 = -\frac{1}{n_0}\frac{T_{e0}}{m_e}\frac{\partial \hat{n}}{\partial x} + \frac{\hat{n}}{n_0^2}\frac{T_{e0}}{m_e}\frac{dn_0}{dx} - \frac{1}{n_0}\frac{\hat{T}_e}{m_e}\frac{dn_0}{dx} - \frac{\partial}{\partial x}\frac{\hat{T}_e}{m_e} + \frac{e}{m_e}\left(\frac{\partial \hat{\phi}}{\partial x} - \hat{v}_{ey}B_0\right) - (n_{n0}\hat{v}_{ex} + \hat{n}_n v_{ex0})\xi_{e0}, \tag{41}$$

$$0 = -\frac{1}{n_0}\frac{T_{e0}}{m_e}\frac{\partial \hat{n}}{\partial y} - \frac{\partial}{\partial y}\frac{\hat{T}_e}{m_e} + \frac{e}{m_e}\left(\frac{\partial \hat{\phi}}{\partial y} + \hat{v}_{ex}B_0\right) - (n_{n0}\hat{v}_{ey} + \hat{n}_n v_{ey0})\xi_{e0}, \tag{42}$$

$$\frac{\partial}{\partial t}\left(\frac{3}{2}\hat{T}_e\right) + \frac{5}{2}\hat{v}_{ex}\frac{dT_{e0}}{dx} + \frac{5}{2}v_{ex0}\frac{\partial \hat{T}_e}{\partial x} + \frac{5}{2}v_{ey0}\frac{\partial \hat{T}_e}{\partial y} - \frac{\hat{n}}{n_0^2}\frac{dq_{ex0}}{dx} + \frac{1}{n_0}\left(\frac{\partial \hat{q}_{ex}}{\partial x} + \frac{\partial \hat{q}_{ey}}{\partial y}\right) = \frac{T_{e0}}{n_0}\frac{\partial \hat{n}}{\partial t} - \hat{n}_n\xi_{ion0}\left(E'_{ion0} + \frac{5}{2}T_{e0}\right) - \frac{5}{2}n_{n0}\xi_{ion0}\hat{T}_e - e\hat{v}_{ex}E_0 + ev_{ex0}\frac{\partial \hat{\phi}}{\partial x} + ev_{ey0}\frac{\partial \hat{\phi}}{\partial y}, \tag{43}$$

$$0 = \frac{5}{2}\hat{n}T_{e0}\frac{dT_{e0}}{dx} + \frac{5}{2}n_0\hat{T}_e\frac{dT_{e0}}{dx} + \frac{5}{2}n_0T_{e0}\frac{\partial\hat{T}_e}{\partial x} + e\hat{q}_{ey}B_0 + m_e\xi_{e0}(\hat{n}_n q_{ex0} + n_{n0}\hat{q}_{ex}), \quad (44)$$

$$0 = \frac{5}{2}n_0T_{e0}\frac{\partial\hat{T}_e}{\partial y} - e\hat{q}_{ex}B_0 + m_e\xi_{e0}(\hat{n}_n q_{ey0} + n_{n0}\hat{q}_{ey}). \quad (45)$$

Once the previous equations are transformed to non-dimensional space, the stability analysis can be formulated as the eigenvalue problem in Eq. (28), where $\tilde{\mathbf{w}}$ is extended with $(\tilde{T}_e, \tilde{q}_{ex}, \tilde{q}_{ey})$ and $\tilde{\mathbf{p}}_0$ with $(\tilde{E}'_{ion0})$. Once again, since electromagnetic and non-quasineutral terms, and electron inertia are not considered, the electron momentum vector equation and the heat flux vector equation, can be pre-eliminated from the matrix formulation.

In this case, no analytical solution is investigated and only the results from the numerical solutions of the corresponding eigenvalue problem are shown. Figures 7 and 8 show the numerical solution of the stability problem for the same case as for the isothermal model. In particular, the growth rate of the most unstable mode and its real part are shown in Fig. 7. It is possible to see that the same long-wavelength instability appears as in the isothermal model. Moreover, as expected, results from the simpler model are recovered if no temperature gradients are assumed for the zero-th order solution. As the temperature gradient increases, the range of azimuthal wave numbers where unstable perturbations exist is reduced. On the other hand, the phase speed of the unstable perturbation is still of the order of the ion acoustic speed and the frequency of the oscillation of the order of 10 kHz. Figure 8 shows the stability map of the perturbation with respect to the temperature and the neutral-to-plasma density ratio. The conclusions are similar to those derived from the isothermal model.

IV. COMPARISON AGAINST PREVIOUS LOCAL STABILITY ANALYSES

The simplified expression derived in the previous section, Eq. (30), may be compared against the one derived by Frias *et al.*[54] in the limit of no ionization. Similar

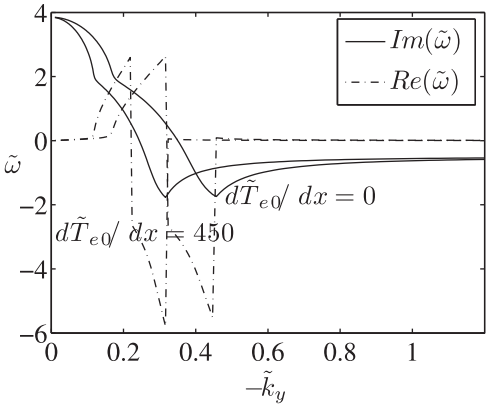

FIG. 7. Growth rate (-) and real part (-·) of the most unstable solution for the following non-dimensional parameters: $\tilde{n}_{n0} = 20$, $\tilde{v}_{ix0} = 5$, $\tilde{v}_{nx0} = 5$, $\tilde{\xi}_{ion0} = 0.5$, $\tilde{\xi}_{e0} = 0$, $\tilde{T}_{e0} = 450$ and $\tilde{B}_0 = 1$. Parametric variation of $\tilde{k}_y$ and $d\tilde{T}_{e0}/dx$.

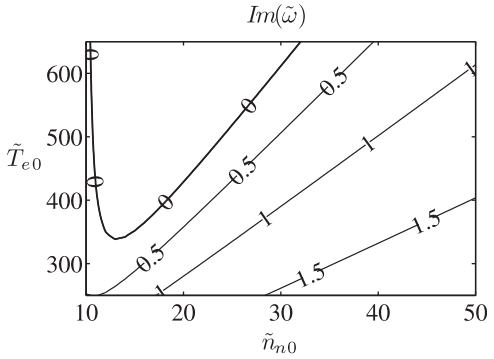

FIG. 8. Growth rate of the most unstable solution for the following non-dimensional parameters: $\tilde{k}_y = -0.25$, $\tilde{v}_{ix0} = 5$, $\tilde{v}_{nx0} = 5$, $\tilde{\xi}_{ion0} = 0.5$, $\tilde{\xi}_{e0} = 0$ and $\tilde{B}_0 = 1$. Parametric variation of $\tilde{n}_{n0}$ and $\tilde{T}_{e0}$, with $\tilde{T}_{e0} = d\tilde{T}_{e0}/d\tilde{x}$.

conclusions could be derived by comparing the expressions obtained in our study against those derived by Morozov *et al.*[12] or Esipchuk and Tilinin.[51] A major difference between the results obtained by Frias *et al.* and those presented here is related to the presence of the magnetic field gradient in the resulting expressions. While the length scale of variation of the magnetic field $(\tilde{l}_B = (Ld\ln B_0/dx)^{-1})$ does not appear in Eq. (30), it plays a major role in the analysis of Frias *et al.* The reason for this, as explained before, is the fact that the equations for the electron axial and azimuthal velocity are replaced by Frias *et al.* in the electron continuity equation before the linearisation and the Fourier-expansion of the equations. In case this approach is used in our analysis, the following expression is obtained under the same hypotheses leading to Eq. (30):

$$0 = \tilde{\omega}^2 + \tilde{\omega}(i\tilde{n}_{n0}\tilde{\xi}_{ion0} - i\tilde{v}_{ix0}/\tilde{l}_n + \tilde{k}_y\tilde{l}_g\tilde{B}_0) + \tilde{n}_{n0}\tilde{\xi}_{ion0}\tilde{v}_{ix0}/\tilde{l}_n - \tilde{k}_y^2\tilde{l}_g\tilde{B}_0(\tilde{v}_{ey0} - 2\tilde{T}_{e0}/(\tilde{l}_B\tilde{B}_0)) - \tilde{k}_y\tilde{l}_g\tilde{B}_0 i\tilde{n}_{n0}\tilde{\xi}_{ion0}, \quad (46)$$

where $1/\tilde{l}_g = 1/\tilde{l}_n - 2/\tilde{l}_B$. In the limit of no ionization and zero ion velocity gradient, Eq. (46) reduces to

$$0 = \tilde{\omega}^2 + \tilde{\omega}\tilde{k}_y\tilde{l}_g\tilde{B}_0 - \tilde{k}_y^2\tilde{l}_g\tilde{B}_0(\tilde{v}_{ey0} - 2\tilde{T}_{e0}/(\tilde{l}_B\tilde{B}_0)) \quad (47)$$

which, aside from the use of non-dimensional variables, is equivalent to the expression derived by Frias *et al.* under the same hypotheses for purely azimuthal oscillations ($\tilde{k}_x = 0$), Eq. (17) of Ref. 54.

The analysis of Eq. (46) shows that in the case of positive gradients $(\tilde{l}_n, \tilde{l}_B > 0)$, apart from the unstable solutions already predicted by Frias *et al.* when $\tilde{l}_B > 2\tilde{l}_n$, there are also unstable solutions when $\tilde{l}_B < 2\tilde{l}_n$ due to the ionization terms. Similar to the unstable solutions given by Eq. (31), the latter unstable solutions from Eq. (46) have also a higher growth rate for smaller wave numbers. This is a distinct feature with respect to the unstable solutions already predicted by Frias *et al.*, for which the higher the wave number is, the higher the growth-rate is. Experiments show that both gradient-induced and spoke oscillations have low wave-numbers and this fact seems to point to the oscillations caused by the ionization terms in Eqs. (31) and (46).

V. CONCLUSIONS

A thorough review of the available literature on low frequency azimuthal oscillations in Hall effect thrusters has been carried out and has justified the need for a stability analysis of the plasma in the ionization region of the channel. The local linear stability has allowed us to identify an azimuthal instability not previously described theoretically in the Hall thruster literature. The linear oscillation is similar to the spokes measured experimentally in terms of frequency range, phase speed, and wavelength. Parametric analyses have been carried out with respect to the main parameters of the model in order to identify the trends of the instability. Moreover, a simplified set of linear differential equations able to reproduce the instability has been derived and analysed, providing some insight into the mechanism of the linear oscillation.

However, the local analysis presented here has limitations that recommend extending the work. The main drawback of the local analysis is related to the fact that axial variations of the zero-th order variables are neglected. This is only valid in the limiting case where the length scale of these variations is much larger than the axial wavelength of the perturbations. In order to overcome this limitation, in Part II of this study a global stability analysis is carried out accounting for the ionization and following an approach similar to those used by Kapulkin *et al.*[45,46] and Litvak *et al.*[44] in the past for other stability studies of the Hall thruster discharge in the high frequency range. Preliminary results from that global approach have already been presented by the authors in Ref. 63.

ACKNOWLEDGMENTS

Support is being provided by the Air Force Office of Scientific Research, Air Force Material Command, USAF, under Grant No. FA8655-13-1-3033. Additional support comes from Spain's R&D National Plan (Project No. AYA-2010-16699).

[1]G. Cann and G. Marlotte, AIAA J. **2**, 1234 (1964).
[2]A. Zharinov and Y. Popov, Sov. Phys.: Tech. Phys. **12**, 208 (1967).
[3]A. Morozov, A. Kislov, and I. Zubkov, ZhETF Pis ma Redaktsiiu **7**, 224 (1968) [7, 172 (1968)]; available at http://www.jetpletters.ac.ru/ps/1683/article_25624.pdf.
[4]M. Martinez-Sanchez and J. Pollard, J. Propul. Power **14**, 688 (1998).
[5]A. Morozov, Y. Esipchuk, G. Tilinin, A. Trofimov, and Y. Sharov, Sov. Phys.: Tech. Phys. **17**, 38 (1972).
[6]N. Meezan and M. Cappelli, "Electron density measurements for determining the anomalous electron mobility in a coaxial Hall discharge plasma," in *Proceedings of the 36th Joint Propulsion Conference* (American Institute of Aeronautics and Astronautics, 2000), A1AA-2000–3420.
[7]N. Meezan, W. Hargus, Jr., and M. Cappelli, Phys. Rev. E **63**, 26410 (2001).
[8]M. Cappelli, N. Meezan, and N. Gascon, "Transport physics in Hall plasma thrusters," in *Proceedings of the 40th AIAA Aerospace and Sciences Meeting and Exhibit* (American Institute of Aeronautics and Astronautics, 2002), AIAA-2002–0485.
[9]J. A. Linnell and A. D. Gallimore, "Hall thruster electron motion characterization based on internal probe measurements," in *Proceedings of the 31st International Electric Propulsion Conference* (Electric Rocket Propulsion Society, 2009), IEPC-2009–105.
[10]C. Boniface, L. Garrigues, G. Hagelaar, J. Boeuf, D. Gawron, and S. Mazouffre, Appl. Phys. Lett. **89**, 161503 (2006).
[11]D. Gawron, S. Mazouffre, and C. Boniface, Plasma Sources Sci. Technol. **15**, 757 (2006).
[12]A. Morozov, Y. Esipchuk, A. Kapulkin, V. Nevrovskii, and V. Smirnov, Sov. Phys.: Tech. Phys. **17**, 482 (1972).
[13]S. Yoshikawa and D. Rose, Phys. Fluids **5**, 334 (1962).
[14]G. Janes and R. Lowder, Phys. Fluids **9**, 1115 (1966).
[15]A. Morozov, Sov. Phys.: Tech. Phys. **32**, 901 (1987).
[16]E. Ahedo, J. Gallardo, and M. Martinez-Sanchez, Phys. Plasmas **10**, 3397 (2003).
[17]L. Garrigues, G. Hagelaar, C. Boniface, and J. Boeuf, J. Appl. Phys. **100**, 123301 (2006).
[18]F. Parra, E. Ahedo, J. Fife, and M. Martinez-Sanchez, J. Appl. Phys. **100**, 023304 (2006).
[19]P. Lomas and J. Kilkenny, Plasma Phys. **19**, 329 (1977).
[20]E. Chesta, C. Lam, N. Meezan, D. Schmidt, and M. Cappelli, IEEE Trans. Plasma Sci. **29**, 582 (2001).
[21]J. Parker, Y. Raitses, and N. Fisch, Appl. Phys. Lett. **97**, 091501 (2010).
[22]Y. Esipchuk, A. Morozov, G. Tilinin, and A. Trofimov, Sov. Phys.: Tech. Phys. **18**, 928 (1974).
[23]W. A. Hargus, N. B. Meezan, and M. A. Cappelli, "A study of a low power hall thruster transient behavior," in *Proceedings of the 25th International Electric Propulsion Conference* (Electric Rocket Propulsion Society, 1997), IEPC-1997-058.
[24]A. Dinklage, T. Klinger, G. Marx, and L. Schweikhard, *Plasma Physics: Confinement, Transport and Collective Effects* (Springer-Verlag, Berlin, 2005).
[25]N. Gascon, N. Meezan, and M. Cappelli, "Low frequency plasma wave dispersion and propagation in Hall thrusters," in *Proceedings of the 27th International Electric Propulsion Conference* (Electric Rocket Propulsion Society, 2001), IEPC-2001-056.
[26]N. Gascon and M. Cappelli, "Wall effects on the excitation and propagation of instabilities in Hall thrusters," in *Proceedings of the 28th International Electric Propulsion Conference* (Electric Rocket Propulsion Society, 2003), IEPC-2003-328.
[27]N. Gascon and M. Cappelli, "Plasma instabilities in the ionization regime of a Hall thruster," in *Proceedings of the 39th Joint Propulsion Conference* (American Institute of Aeronautics and Astronautics, 2003), AIAA-2003-4857.
[28]A. Smith and M. Cappelli, "Time and space-correlated plasma property measurements in the near-field of a coaxial hall discharge," in *Proceedings of the 31st International Electric Propulsion Conference* (Electric Rocket Propulsion Society, 2009), IEPC-2009-135.
[29]Y. Raitses, A. Smirnov, and N. Fisch, Phys. Plasmas **16**, 057106 (2009).
[30]C. L. Ellison, Y. Raitses, and N. J. Fisch, "Direct measurement of spoke-induced, cross-field electron current in a cylindrical Hall thruster," in *Proceedings of the 32nd International Electric Propulsion Conference* (Electric Rocket Propulsion Society, 2011), IEPC-2011-173.
[31]C. Ellison, Y. Raitses, and N. Fisch, IEEE Trans. Plasma Sci. **39**, 2950 (2011).
[32]C. Ellison, Y. Raitses, and N. Fisch, Phys. Plasmas **19**, 013503 (2012).
[33]Y. Raitses, M. Griswold, L. Ellison, J. Parker, and N. Fisch, in *Proceedings of the 48th Joint Propulsion Conference* (American Institute of Aeronautics and Astronautics, 2012), AIAA-2012-4179.
[34]M. Griswold, C. Ellison, Y. Raitses, and N. Fisch, Phys. Plasmas **19**, 053506 (2012).
[35]Y. Shi, Y. Raitses, and A. Diallo, "Driving azimuthal modes in magnetized discharge with segmented anode," in Proceedings of the 4th Annual Meeting, DOE Center for Predictive Control of Plasma Kinetics, 2013.
[36]M. McDonald, C. Bellant, B. Pierre, and A. Gallimore, "Measurement of cross-field electron current in a Hall thruster due to rotating spoke instabilities," in *Proceedings of the 47th Joint Propulsion Conference* (American Institute of Aeronautics and Astronautics, 2011), AIAA-2011-5810.
[37]M. S. McDonald and A. D. Gallimore, "Parametric investigation of the rotating spoke instability in Hall thrusters," in *Proceedings of the 32nd International Electric Propulsion Conference* (Electric Rocket Propulsion Society, 2011), IEPC-2011-242.
[38]M. S. McDonald and A. D. Gallimore, IEEE Trans. Plasma Sci. **39**, 2952 (2011).
[39]M. Sekerak, M. McDonald, R. Hofer, and A. Gallimore, "Hall thruster plume measurements from high-speed dual langmuir probes with ion saturation reference," in *2013 IEEE Aerospace Conference* (IEEE, 2013), pp. 1–16.

[40]D. Liu, "Two-dimensional time-dependent plasma structures of a Hall-effect thruster," Ph.D. dissertation (Standford University, 2011).
[41]D. Liu, R. Huffman, R. Branam, and W. Hargus, IEEE Trans. Plasma Sci. **39**, 2926 (2011).
[42]C. M. Lam, A. K. Knoll, M. A. Cappelli, and E. Fernandez, "Two-dimensional (z-θ) simulations of Hall thruster anomalous transport," in *Proceedings of the 31st International Electric Propulsion Conference* (Electric Rocket Propulsion Society, 2009), IEPC-2009-102.
[43]J. Fife, "Hybrid-PIC modelling and electrostatic probe survey of Hall thrusters," Ph.D. dissertation (Massachusetts Institute of Technology, 1998).
[44]A. Litvak and N. Fisch, Phys. Plasmas **11**, 1379 (2004).
[45]A. Kapulkin and V. Prisnyakov, "Dissipative method of suppression of electron drift instability in SPT," in *Proceedings of the 24th International Electric Propulsion Conference* (Electric Rocket Propulsion Society, 1995), IEPC-1995-037.
[46]A. Kapulkin, J. Ashkenazy, A. Kogan, G. Appelbaum, D. Alkalay, and M. Guelman, "Electron instabilities in Hall thrusters: modelling and application to electric field diagnostics," in *Proceedings of the 28th International Electric Propulsion Conference* (Electric Rocket Propulsion Society, 2003), IEPC-2003-100.
[47]A. Kapulkin and M. Guelman, "Lower-hybrid instability in Hall thruster," in *Proceedings of the 29th International Electric Propulsion Conference* (Electric Rocket Propulsion Society, 2005), IEPC-2005-088.
[48]H. K. Malik and S. Singh, Phys. Rev. E **83**, 036406 (2011).
[49]A. Nelson and M. Haines, Plasma Phys. **11**, 811 (1969).
[50]A. Simon, Phys. Fluids **6**, 382 (1963).
[51]Y. Esipchuk and G. Tilinin, Sov. Phys.: Tech. Phys. **21**, 417 (1976).
[52]A. Kapulkin and M. Guelman, "Low frequency instability and enhanced transfer of electrons in near-anode region of Hall thruster," in *Proceedings of the 30th International Electric Propulsion Conference* (Electric Rocket Propulsion Society, 2007), IEPC-2007-079.
[53]A. Kapulkin and M. M. Guelman, IEEE Trans. Plasma Sci. **36**, 2082 (2008).
[54]W. Frias, A. I. Smolyakov, I. D. Kaganovich, and Y. Raitses, Phys. Plasmas **19**, 072112 (2012).
[55]A. Smolyakov, W. Frias, Y. Raitses, and N. J. Fisch, "Gradient instabilities in Hall thruster plasmas," in *Proceedings of the 32nd International Electric Propulsion Conference* (Electric Rocket Propulsion Society, 2011), IEPC-2011-271.
[56]W. Frias, A. I. Smolyakov, I. D. Kaganovich, and Y. Raitses, Phys. Plasmas **20**, 052108 (2013).
[57]E. Chesta, N. Meezan, and M. Cappelli, J. Appl. Phys. **89**, 3099 (2001).
[58]J. Gallardo and E. Ahedo, "On the anomalous diffusion mechanism in Hall-effect thrusters," in *Proceedings of 29th International Electric Propulsion Conference* (Electric Rocket Propulsion Society, 2005), IEPC-2005-117.
[59]H. K. Malik and S. Singh, Phys. Plasmas **20**, 052115 (2013).
[60]S. Barral, K. Makowski, Z. Peradzyński, and M. Dudeck, Phys. Plasmas **12**, 073504 (2005).
[61]E. Choueiri, Phys. Plasmas **8**, 1411 (2001).
[62]G. Tilinin, Sov. Phys.: Tech. Phys. **22**, 974 (1977).
[63]D. Escobar and E. Ahedo, "Global stability analysis of azimuthal oscillations in Hall thrusters," in *Proceedings of the 33rd International Electric Propulsion Conference* (Electric Rocket Propulsion Society, 2013), IEPC-2013-304.

AIP | Physics of Plasmas

Low frequency azimuthal stability of the ionization region of the Hall thruster discharge. I. Local analysis

D. Escobar and E. Ahedo

Citation: Physics of Plasmas (1994-present) **21**, 043505 (2014); doi: 10.1063/1.4870963
View online: http://dx.doi.org/10.1063/1.4870963
View Table of Contents: http://scitation.aip.org/content/aip/journal/pop/21/4?ver=pdfcov
Published by the AIP Publishing